
*17th World Conference on Earthquake Engineering, 17WCEE*
*Sendai, Japan - September 13th to 18th 2020*

# EXPERIMENTAL STUDY ON BOND SPLIT FAILURE OF TENSION REINFORCING BARS EMBEDDED IN CONCRETE

K. Nishimura[(1)], N. Onishi[(2)], M. Kawazu[(3)]

[(1)] *Associate Professor, Tokyo Institute of Technology, nishimura.k.ac@m.titech.ac.jp*
[(2)] *Assistant Professor, The University of Tokyo, onishi@arch.t.u-tokyo.ac.jp*
[(3)] *Former Graduate Student, Graduate School of Engineering, Hokkaido University*

## *Abstract*

There have been many pull-out tests of single and double layered deformed bars to investigate bond strength in R/C members. In Japan, it is required to check bond stress around each deformed bar in RC beams and columns. Bond strength formula is provided for three bond split modes: side split, corner split, and V-notch split modes. The bond strength of a tension reinforcing bar in multi-layers is influenced by bond stress transferred from adjacent bars. Therefore, the bond strength is reduced by 40% when the strengths of inner bars in multi-layers are calculated in accordance with AIJ Standard provided by Architectural Institute of Japan. However, it is difficult to evaluate the bond strength with good accuracy because it is necessary to evaluate the bond stress of adjacent bars for calculating the bond strength of the bar in question.

In order to evaluate the bond capacities of multi-layered reinforcing bars, a new method was proposed in previous study. This method is for evaluating total bond capacity on the side split mode, and can be applied to multi-layered tension reinforcement. Because a longitudinal bar may fail in bond individually, the bond stress must also be checked to prevent local bond failure. The corner split and the V-notch split modes can be classified as the local bond failure. The local bond failure does not necessarily cause decrease in capacity of the beam if the other bars than the failing bar keep their performance, though the beam cannot perform as expected in the flexural capacity. On the other hand, entire bond failure like the side split mode causes decrease in the capacity of the beam, thus the author used the total bond capacity for evaluating shear capacity of the beam. In the previous study, to evaluate strength on the local bond failure, the authors conducted pull-out tests of deformed bars straightly embedded in concrete. The test results were classified into entire bond failure and local bond failure. It was implied that split modes in which more than one bar split concrete for upper side or lateral side occurred. We proposed a new method to evaluate strengths on the local bond failure (top split mode and lateral split mode) and a way to expect the split mode were proposed. In the bond strength formulas, split lines in which more than one bar split concrete for upper side or lateral side were assumed.

In this paper, the methods for calculating the total bond capacity and the bond strength under the local bond failure are reviewed first, and a discussion on bond strength of lightweight concrete is added. The effect of concrete weight was considered in those calculation methods. Calculated values and failure modes according to the proposed method successfully agreed with the results of pull-out tests of deformed bars embedded in concrete. This result implies that the local bond failure can be prevented by using the total bond capacity and the bond strengths of the local bond failure.

*Keywords: reinforced concrete, deformed bar, bond strength, double layers, local failure*



## 1. Introduction

The Architectural Institute of Japan (AIJ) provides standards and guidelines for the design of buildings in Japan. When designers examine structural performance of a reinforced concrete (RC) building in Japan, they follow the AIJ's "RC Standard [1]" and "Inelastic Concept Guidelines [2]". When a RC flexural member is designed in accordance with these documents, bond stress around each reinforcing bar in the member is checked to determine the development length of the bar.

In the RC Standard, three bond split modes are assumed (see Fig.1), and the bond strength formulas are provided for individual longitudinal bars. One of the authors claimed that the side split failure must be prevented by evaluating the total bond capacity of the longitudinal bars, especially multi-layered longitudinal bars [3, 4]. This means evaluating shear strength on a failure section due to bond splitting as shown in Fig.2. It is known that the bond strength of individual bars is influenced by bond stress from adjacent bars. Because the inner (second) bars usually have weaker bond strength than the outer (first) bars, the bond strength in the second layer is reduced by 40% in the RC Standard and the Inelastic Concept Guidelines. However, in previous loading test of RC beams with double layered bars [5], cut-off bars in the second layer have been observed higher bond strength than those of bars passing though the span from end to end. This is because that terminating the inner (second) bars reduces bond stress around the bars in the first layer in the range of the double layers [3]. Because differences in bar arrangement influence bond stress of adjacent bars, evaluating the bond strength of individual bar is difficult. Thus, one of the authors proposed a method for calculating total bond capacity of tension longitudinal bars, and showed the calculated values agreed with the experimental values [3, 4].

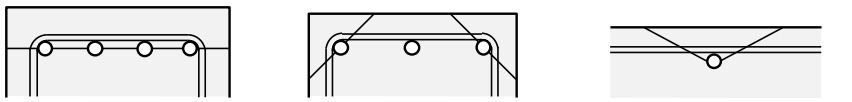

(a) Side split mode (b) Corner split mode (c) V-notch split mode

Fig. 1 – Bond split modes [1]

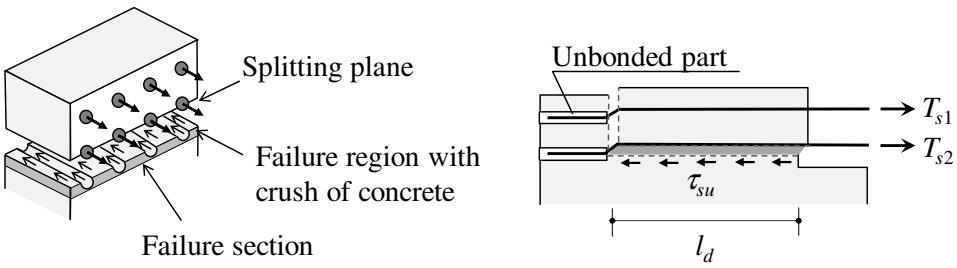


(a) Failure section (b) Shear strength on failure section, $\tau_{su}$

Fig. 2 – Failure section and definition of strength [3]

Because a longitudinal bar may fail in bond individually, the bond stress must also be checked to prevent local bond failure. The corner split and the V-notch split modes (see Fig.1) can be classified as the local bond failure. The local bond failure does not necessarily cause decrease in capacity of the beam if the other bars than the failing bar keep their performance [6], though the beam cannot perform as expected in the flexural capacity. On the other hand, entire bond failure like the side split mode causes decrease in the capacity of the beam, thus the author used the total bond capacity for evaluating shear capacity of the beam [3]. In the previous study [7], to evaluate strength on the local bond failure, the authors conducted pull-out tests of deformed bars straightly embedded in concrete. The test results were classified into entire bond failure and local bond failure. It was implied that split modes in which more than one bar split concrete for upper side or lateral side occurred



 



in the local bond failure. We proposed a new method to evaluate strengths on the local bond failure and a way to expect the failure mode [7].

In this paper, the methods for calculating the total bond capacity [3, 4] and the bond strength under the local bond failure [7] are reviewed first, and a discussion on bond strength of lightweight concrete is added.

## 2. Total Bond Capacity

### 2.1 Influence of bond stress in first layer on side splitting at second layer

There have been many pullout tests of longitudinal bars arranged in single and double layers like those shown in Fig3. Fig.4 shows how bond strengths around bars in the second layer are influenced by bond stresses in the first layer. Here, bond strength of bars in the second layer ($\tau_{bu2}$) and shear strength ($\tau_{su}$) are plotted against the ratio of tensile force in the first layer to that in the second layer ($T_{s1}/T_{s2}$). The data used to create Fig.4 come from tests by Masuda et al. [8] on pullout specimens with two bars in the first layer, three bars in the second layer, and no transverse reinforcement (summarized in Table 1). Fig.2a shows a region of failure and the difference between a splitting plane and a failure section. Slip of the bars after splitting begins causes crushing of the surrounding concrete, shown by the darkened region below the splitting plane in Fig.2a. The failure section is assumed to lie below the bottom of the failure region. Shear stress on the failure section is defined as shown in Fig.2b, with shear strength denoted as $\tau_{su}$. Average bond stress is defined as shown in Fig.3, with bond strength denoted as $\tau_{bu}$. All the specimens shown in Fig.4 failed in bond-splitting in the second layer. Although $\tau_{bu}$ decreases as the $T_{s1}/T_{s2}$ decreases, $\tau_{su}$ maintains nearly constant strength when $T_{s1}/T_{s2}$ is larger than 0.3. This result implies that shear strength on a failure section at the second layer in a beam may be constant even if bond stress around the first layer changes.

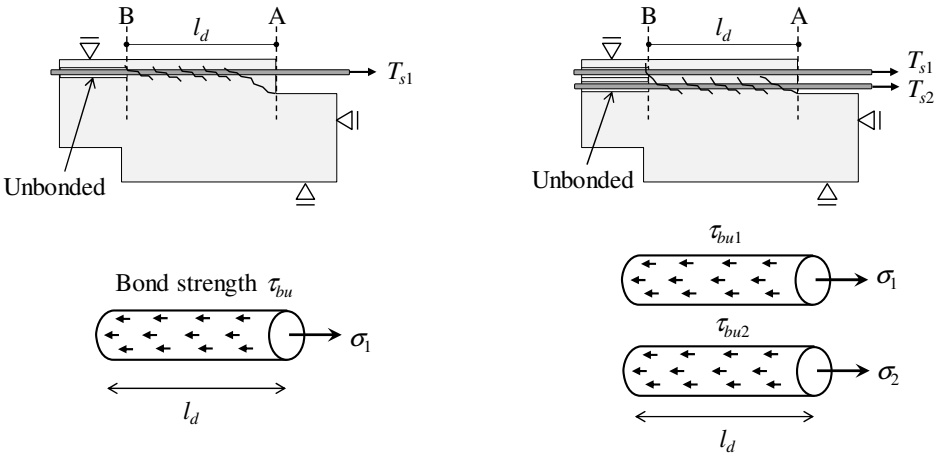


(a) Single layered bars (b) Double layered bars

Fig. 3 – Pullout test of longitudinal bars embedded in concrete

### 2.2 Difference of bond strength between single and double layers

Difference of $\tau_{su}$ between single and double layers of reinforcement is examined. In Fig.5, the vertical axis is $\tau_{su}$ and the horizontal axis is transverse reinforcement ratio, $\rho_t$. Transverse reinforcement ratio is defined as $\rho_t = a_w/(bs)$, where $a_w$ is cross-sectional area of the transverse bars crossing horizontal section of $bs$, $b$ is beam width, and $s$ is spacing of the transverse reinforcement. “Top” and “bottom” in Fig.5 refer to locations of the longitudinal bars with reference to the casting direction of concrete. Lightweight concrete with a specified



 



compressive strength of $f'_c$=36 MPa was used for the specimens so that the bond strengths would be smaller. Other properties of the specimens are summarized in Table 1 (see Ref.9). As shown in Fig.5, the shear strengths ($\tau_{su}$) of the top bars were observed to be smaller than those of the bottom bars. And the shear strengths of the double-layered specimens were larger than those of the single-layered specimens.

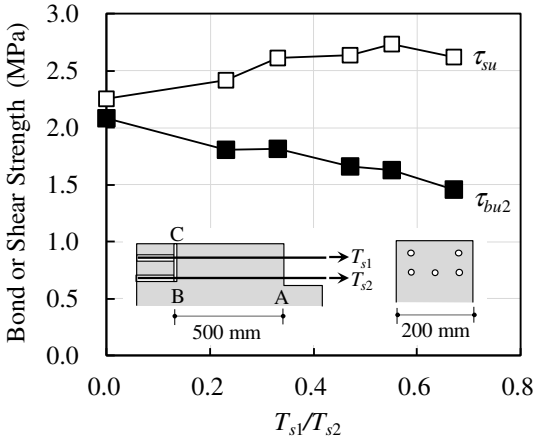


Fig. 4 – Influence of tensile force in first layer

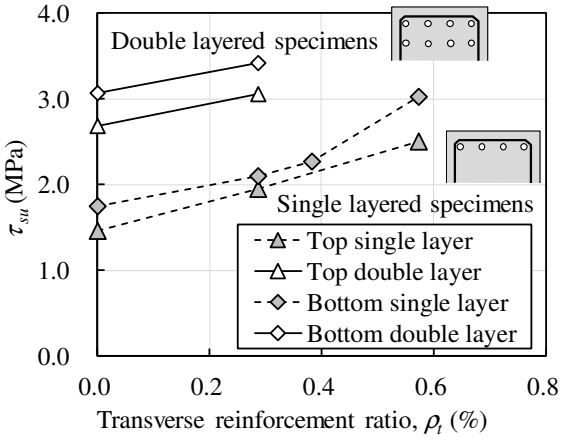


Fig. 5 – $\tau_{su}$ of single and double layered specimens

## 2.3 Effect of transverse reinforcement

Regarding the effect of transverse reinforcement in Fig.5, the slope of $\tau_{su}$ with respect to $\rho_t$ is almost the same even if the number of layers and the location of the bars are different. This trend is important because it shows that shear strength varies similarly with transverse reinforcement ratio whether the bars are in a single layer or in two layers, although their "base" shear strengths at $\rho_t$ =0% may differ. Similar results can be seen in Fig.6, where the axes are the same as Fig.5, but the test data come from different specimens (Ref.4 in Table 1). These specimens were made of normal-weight concrete with a range of compressive strengths. The top bar effect was not considered for these specimens because of a shallower casting depth of concrete, where the concrete was cast in the same direction as the specimen width of 200 mm. Fig.6 shows similar trends as Fig.5 regarding the slope of $\tau_{su}$ with respect to $\rho_t$, but it also shows that the slopes are similar even if the concrete strengths are different.

## 2.4 Bond strength of light weight concrete

Fig.7 shows how concrete weight affects the slope of $\tau_{su}$ with respect to $\rho_t$, where the axes and the markers of the specimens are the same as in Figs.5 and 6. At a reinforcement ratio of 0.2%, the curves for lightweight concrete and normal-weight concrete intersect, but the strength of the lightweight concrete was 36 MPa compared with 21-24 MPa for the normal-weight concrete. This suggests that the shear strength of lightweight concrete will be smaller than that of normal-weight concrete of the same compressive strength. In addition, as shown in Fig.7, the slopes of shear strength with respect to transverse reinforcement ratio for lightweight concretes are shallower than those for normal-weight concrete: that is, transverse reinforcement may be less effective at increasing shear strength in lightweight concrete.

## 2.5 Bond capacity formula

The above observations can be summarized as follows: (1) Bond strength ($\tau_{bu}$) in the second layer is sensitive to bond stress in the first layer, but shear strength ($\tau_{su}$) is insensitive to changes in bond stress in the first layer; (2) While $\tau_{su}$ of the double-layered specimens are larger than those of the single-layered specimens, the slopes of $\tau_{su}$ with respect to $\rho_t$ are almost the same even if the number of layers, casting location of the bars, and concrete strength are different; (3) The $\tau_{su}$ of lightweight concrete is lower than that of normal weight-concrete



 



of the same concrete strength. In addition, the slope of $\tau_{su}$ with respect to $\rho_t$ of lightweight concrete is shallower than that of normal-weight concrete.

Table 1 – Test data of pullout tests in previous study, part 1

| Ref. No. | Name of specimen | $f_{cm}$,† MPa | $b$, mm | Transverse reinforcement* | Longitudinal bars* | |
|---|---|---|---|---|---|---|
| | | | | | 1st layer | 2nd layer |
| 8 | DCL0-0 | 35.6 | 200 | $\rho_t$= 0 % | 2-D23, $l_d$=500mm. | 3-D23, $l_d$=500mm. |
| | DCL23-0 | | | | | |
| | DCL33-0 | 37.7 | | | | |
| | DCL47-0 | | | | | |
| | DCL55-0 | | | | | |
| | DCL67-0 | | | | | |
| 9 | No.2T | 39.4 lightweight | 415 | 2-D10@60mm, $\rho_t$= 0.57 % | 4-D29, top bar, $l_d$=580mm. | N/A |
| | No.11T | 38.2 lightweight | | $\rho_t$= 0 % | | |
| | No.12T | | | 2-D10@120mm, $\rho_t$= 0.29 % | | |
| | No.13T | | | 2-D10@90mm, $\rho_t$= 0.38 % | | |
| | No.15T | | | $\rho_t$= 0 % | | 4-D29, top bar, $l_d$=580mm. |
| | No.16T | | | 2-D10@120mm, $\rho_t$= 0.29 % | | |
| | No.2B | 39.4 lightweight | | 2-D10@60mm, $\rho_t$= 0.57 % | 4-D29, $l_d$=580mm. | N/A |
| | No.11B | 38.2 lightweight | | $\rho_t$= 0 % | | |
| | No.12B | | | 2-D10@120mm, $\rho_t$= 0.29 % | | |
| | No.13B | | | 2-D10@90mm, $\rho_t$= 0.38 % | | |
| | No.15B | | | $\rho_t$= 0 % | | 4-D29, $l_d$=580mm. |
| | No.16B | | | 2-D10@120mm, $\rho_t$= 0.29 % | | |
| 4 | 2C3C3-F21 | 22.4 | 200 | 2-D6@160mm, $\rho_t$= 0.20 % | 3-D19, $l_d$=500mm. | 3-D19, $l_d$=500mm. |
| | 2C3C3-F24 | 25.3 | | | | |
| | 2C3C3-F36 | 37.3 | | | | |
| | 4C3C3-F24 | 27.3 | | 2-D6@80mm, $\rho_t$= 0.40 % | | |
| | 6C3C3-F24 | 26.2 | | 2-D10@118mm, $\rho_t$= 0.60 % | | |
| | 2C3-F21 | 20.1 | | 2-D6@160mm, $\rho_t$= 0.20 % | 3-D19, $l_d$=500mm. | N/A |
| | 2C3-F36 | 37.0 | | | | |
| | 2C3-F54 | 52.7 | | | | |
| | 4C3-F21 | 20.1 | | 2-D6@80mm, $\rho_t$= 0.40 % | | |
| | 4C3-F36 | 37.0 | | | | |
| | 4C3-F54 | 52.7 | | | | |

*Bar designation numbers following "D" are nominal diameters in millimeter; "top bar" means bars near top surface of concrete in casting direction.

† Measured compressive strength of concrete cylinder; "lightweight" means light weight concrete and others are normal weight concrete.

Notes: $b$ is width of specimen; $\rho_t$ is transverse reinforcement ratio; $l_d$ is embedment length of the bars.



 



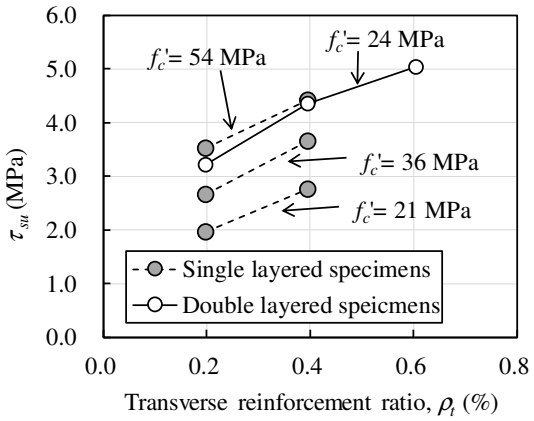


Fig. 6 – Influence of concrete strength

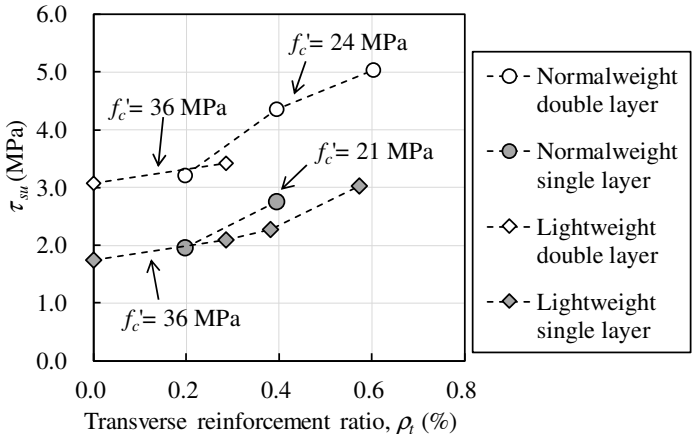


Fig. 7 – Influence of concrete weight

Considering the observations above, a formula was developed for estimating shear stress, $\tau_{su}$. First, we transformed the bond strength formula in the AIJ Guidelines [2] into a shear strength formula. Next, we extend the formula for double-layered arrangements [3, 4]. Then, the influence of concrete weight is considered in this paper. The following equation gives a shear capacity ($\Delta T_{shear}=\tau_{su}bL$) on the failure section.

$$\Delta T_{shear} = \lambda\alpha_t(\tau_{suC} + \tau_{suT}) \times bL \quad (1)$$

$$\tau_{suC} = 0.33\alpha\sqrt{f_c'} \quad (2)$$

$$\tau_{suT} = 180 \times (1.2 + \gamma)\rho_t \quad (3)$$

$$\alpha = \text{min.}\,(1 + a_2/a_1\,, 1.5) \quad (4)$$

$$\gamma = N_t/N \quad (5)$$

In the Eq. (1), $\tau_{suC}$ and $\tau_{suS}$ are contributions of concrete and transverse reinforcement, respectively, in N/mm$^2$. The other symbols are the followings: $\alpha_t$ is a reduction factor for top bar where $\alpha_t$ =min. (0.75+$f_c$'/400, 1.00); $b$ is member width; $L$ is bond length where it is the same as $l_d$ in the pullout tests; $\lambda$ is a reduction factor for light weight concrete where $\lambda$=0.8 which is applied in the RC Standard [1]; $f_c$' is concrete strength in N/mm$^2$; $\alpha$ is an increment factor for multi-layers of longitudinal bars; $\gamma$ is an addition factor of effect of inner ties. The symbols $a_1$ and $a_2$ in the equation (4) are cross sectional areas of the longitudinal bars in first and second layers, respectively. The factor $\gamma$ is calculated by the equation (5), where $N$ is the number of all the longitudinal bars, and $N_t$ is the number of the longitudinal bars with the transverse reinforcement next to it. Fig.8 shows how to count the numbers of $N$ and $N_t$, and how to calculate $\gamma$.

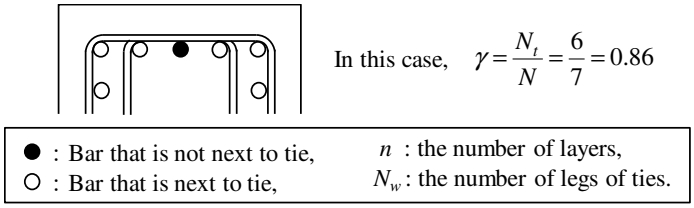


Fig. 8 – Calculation of $\gamma$



 



## 3. Local Bond Failure

### 3.1 Top split failure

We conducted pullout tests of longitudinal bars and discussed local bond failures in the previous study [7]. In the local bond failure, some bars near the concrete surface fail although the other bars still work in bond.

Fig.9 shows pull-out test results of specimens with single layered bars. Test parameters of the single layered specimens were the transverse reinforcement ratio (0.25% and 0.51%) and yield strength of the transverse reinforcement (SD295, 345, and 685), and six combinations of these parameters were prepared (see Table 2). In spite of different transverse reinforcement ratio and yield strengths, the peaks of tensile force ($T_{s1}$) of six specimens are almost the same, where all the transverse reinforcement did not yield at the peak. Fig.10 shows a result of relationships between bond stress and pullout displacement ($\delta_{1ave}$) of the specimen 5.1t2s295-C5. The specimen has five longitudinal bars, hoops, and no inner ties. The bars failed in bond at the peak are painted black in the cross section in Fig.10. Corner longitudinal bars in the specimen failed after the peak. It is thought that influence of the transverse reinforcement on confining the inner three bars is small, and the inner three longitudinal bars splitted concrete upward. We call this failure mode a top split mode.

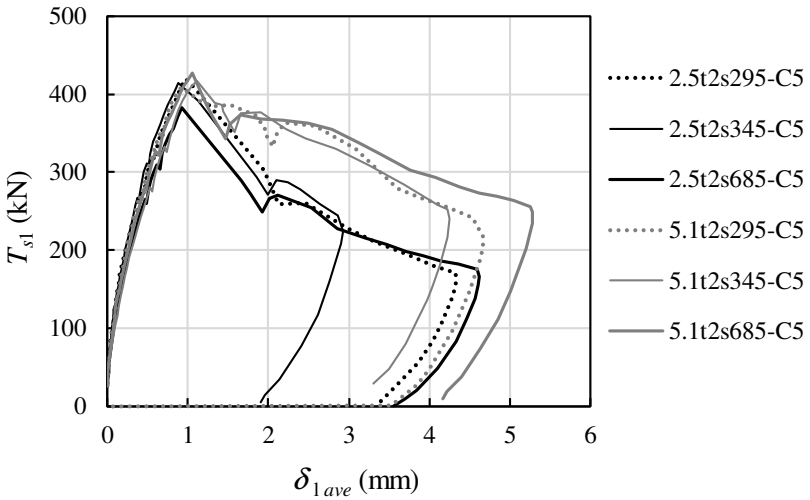


Fig. 9 – Total tensile force – pullout displacement curves

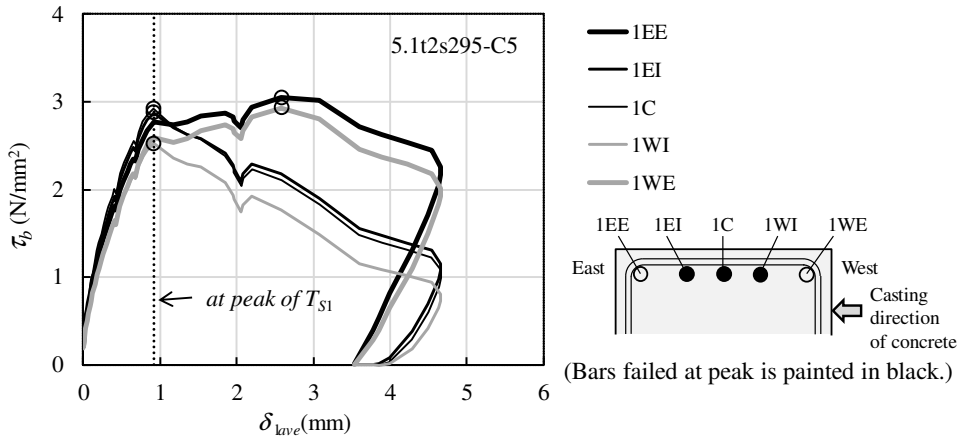


Fig. 10 – Bond stress – pullout displacement curves of single layered specimen



 



Table 2 – Test data of pullout tests in previous study, part2

| Ref. No. | Name of specimen | $f_{cm}$,† MPa | $b$, mm | Transverse reinforcement* | Longitudinal bars* | |
|---|---|---|---|---|---|---|
| | | | | | 1st layer | 2nd layer |
| 7 | 2.5t2s295-C5 | 25.8 | 350 | 2-D10@160mm, $\rho_t$= 0.25 % | 5-D19, $l_d$=500mm. | N/A |
| | 2.5t2s345-C5 | | | | | |
| | 2.5t2s685-C5 | 26.8 | | | | |
| | 5.1t2s295-C5 | 25.8 | | 2-D10@80mm, $\rho_t$= 0.51 % | | |
| | 5.1t2s345-C5 | | | | | |
| | 5.1t2s685-C5 | 26.8 | | | | |
| | 4.0t2-C4C4 | 30.7 | | 2-D6@45mm, $\rho_t$= 0.40 % | 4-D19, $l_d$=500mm. | 4-D19, $l_d$=500mm. |
| | 4.0t2-C4C2 | 30.3 | | | | 2-D19, $l_d$=500mm. |
| | 4.0t3-C5C3 | 28.2 | | 3-D6@68mm, $\rho_t$= 0.40 % | 5-D19, $l_d$=500mm. | 3-D19, $l_d$=500mm. |
| | 4.0t3-C5C2 | 26.6 | | | | 2-D19, $l_d$=500mm. |
| | 4.0t4-C4C4 | 30.2 | | 4-D6@90mm, $\rho_t$= 0.40 % | 4-D19, $l_d$=500mm. | 4-D19, $l_d$=500mm. |
| | 4.0t4-C4C2 | 30.3 | | | | 2-D19, $l_d$=500mm. |
| 9 | No.1T | 39.4 light weight | 415 | 4-D10@120mm, $\rho_t$= 0.57 % | 4-D29, top bar, $l_d$=580mm. | N/A |
| | No.17T | 38.2 light weight | | | | 4-D29, top bar, $l_d$=580mm. |
| | No.1B | 39.4 light weight | | | 4-D29, bottom bar, $l_d$=580mm. | N/A |
| | No.17B | 38.2 light weight | | | | 4-D29, bottom bar, $l_d$=580mm. |

Note: symbols are the same as Table 1.

### 3.2 Lateral split failure

Fig.11 shows test results of specimens with double layered bars. Primary test parameters of the six double layered specimens were the number of inner transverse ties and whether longitudinal bars were placed inside of second layer or not (summarized in Table 2). The transverse reinforcement ratio ($\rho_t$) of every double layered specimen is 0.40%, and the spacing of transverse reinforcement is adjusted according to the number of inner ties. As shown in Fig.11a, in the specimens 4.0t2-C4C2, some bars did not fail in bond at the peak of $T_{s1}$+$T_{s2}$ (see Fig.3b), and the failed bars were not symmetry (see Fig.11a, where the bars failed in bond at the peak are painted black). It is though that this is a combination failure of the side split and the top split modes.

Meanwhile, all the bars in the specimen 4.0t4-C4C2 failed at the peak of $T_{s1}$+$T_{s2}$ (see Fig.11b). Because these specimens were placed transverse reinforcement by the same $\rho_t$, there are fewer perimeter ties in 4.0t4-C4C2 than those in 4.0t2-C4C2. It is thought that bond around the side longitudinal bars in 4.0t4-C4C2 is lower than that in 4.0t2-C4C2 due to the decreased perimeter ties, and the side two longitudinal bars splitted concrete. We call this failure mode a lateral split mode. It is though that the failure mode shown in Fig.11b is a combination failure of the side split and the lateral split modes.



 



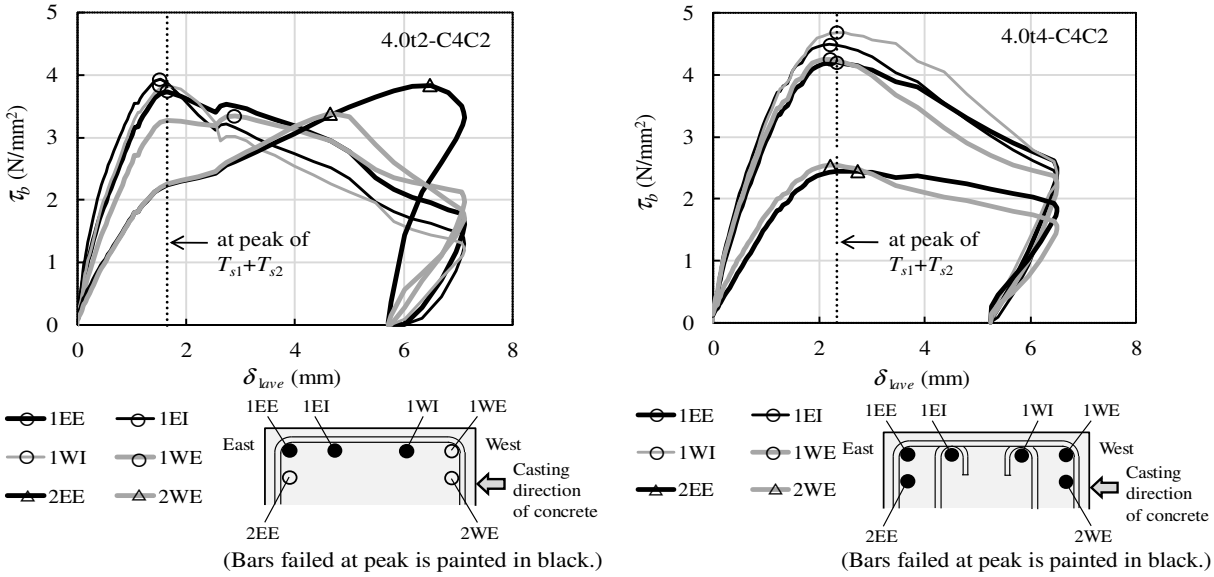


(a) 4.0t2-C4C2 (b) 4.0t4-C4C2

Fig. 11 – Bond stress – pullout displacement curves of double layered specimens

### 3.3 Bond strength formula

We assumed split lines such as Fig.12 to calculate bond strengths of the lateral split and the top split mode [7]. As we derive the bond strength formulas for these split modes, we develop the methods for the split mode shown in Fig.1a to1c by using the bond strength formulas given in the Inelastic Concept Guidelines [2]. Here, the symbols in Fig.12 are as follows: $C_b$ is cover thickness of concrete from the top surface (or the bottom surface); $C_{min}$ is the minimum of cover thicknesses; $C_n$ is clear spacing between the longitudinal bars; $C_s$ is cover thickness from the side surface; $d_b$ is a diameter of longitudinal bars; $N'$ is the number of longitudinal bars on the split line; $N_w'$ is the number of transverse reinforcing bars crossing the split line. The following bond strength formula is given by considering the effect of concrete weight.

$$\tau_{bu} = \lambda \alpha_t \left\{ (0.106 b_i + 0.125)\sqrt{f_c'} + 1.25 k_{st} \right\} \tag{6}$$

$$_{top}b_i = \sqrt{3}\left(\frac{2C_{min}}{N'd_b} + \frac{1}{N'}\right) + \frac{\sum C_n}{N'd_b} \tag{7}$$

$$_{top}k_{st} = \left(54 + 45 \times \frac{N_t'}{N'}\right)\frac{N_w' A_w}{sN'd_b} \tag{8}$$

$$_{lateral}b_i = \sqrt{2}\left(\frac{C_s + C_b + \sum C_n/2}{N'd_b} + \frac{1}{2N'} + \frac{1}{2}\right) - 1 \tag{9}$$

$$_{lateral}k_{st} = 108 \times \frac{A_w}{sN'd_b} \tag{10}$$

In Eq. (6), $b_i$ is a ratio of length of the split line per one longitudinal bar to the bar diameter ($d_b$), and the term $k_{st}$ represents the effect of the transverse reinforcement. The bond strength for the top split mode ($_{top}\tau_{bu}$) is calculated by substituting $_{top}b_i$ and $_{top}k_{st}$ given by Eq. (7) and (8) for $b_i$ and $k_{st}$ in Eq. (6). The strength for the lateral split mode ($_{lateral}\tau_{bu}$) is calculated by substituting $_{lateral}b_i$ and $_{lateral}k_{st}$ given by Eq. (9) and (10) for $b_i$ and $k_{st}$ in Eq. (6). When there is one longitudinal bar on the split line ($C_n$=0 in Fig.12), $_{top}\tau_{bu}$ and $_{lateral}\tau_{bu}$ are agree with bond strengths of the V-notch split mode and the corner split mode (see Fig.1b and 1c), respectively. The



 



symbols in above equations are as follows: $A_w$ is cross sectional area of one transverse reinforcing bar; $N_t$' is the number of the longitudinal bars which are on the split line and next to the transverse reinforcement; $s$ is spacing between center-to-center of transverse reinforcing bars in the direction of member axis; and the other symbols are the same as the above mentioned.

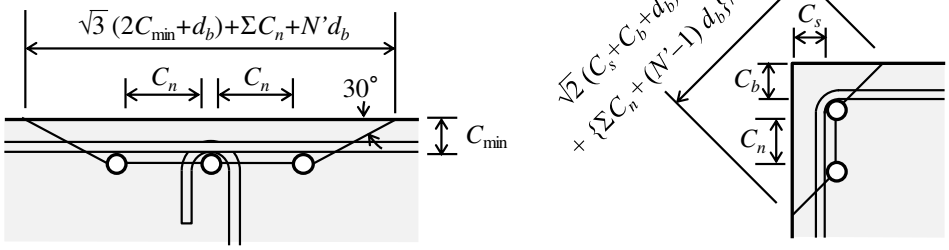


(a) Top split mode (b) Lateral split mode

Fig. 12 – Split line

## 4. Evaluation of Side Split Capacity and Prevention of Local Bond Failure

In the previous study [7], the authors proposed a manner that the side split failure is evaluated by the total bond capacity ($\Delta T_{shear}$), and the local bond failure is evaluated by the bond strength of each longitudinal bar. Here, we verify the accuracy of the calculation method including the effect of concrete weight by using the test data shown in Table 1 and Table 2 except the specimens in the Ref.8.

Total bond forces when the specimens fail due to top splitting or lateral splitting are calculated by using stress distribution shown in Fig.13. The stress distributions are in accordance with loading setup in the tests. $\Delta T_{top}$ is the total bond force for the top split mode where the tensile stress $\sigma_{t1}$ of the bar in the first layer is calculated from the bond strength ($_{top}\tau_{bu}$) of the top split mode. $\Delta T_{lateral}$ is the total bond force for the lateral split mode where the average ($\sigma_{t1\text{-}2}$) of the tensile stresses of the bars in the first and second layers is calculated from $_{lateral}\tau_{bu}$ of the lateral split mode. And the smaller of $\Delta T_{top}$ and $\Delta T_{lateral}$ is defined as the total bond force of the local bond failure ($\Delta T_{local}$). The calculated values are compared with the experimental values in Fig.14. The vertical axis is the experimental value ($T_{sMAX}$) which is the maximum of $T_{s1}+T_{s2}$, the horizontal axis is the calculated value ($\Delta T_{local}$), and both are divided by $\Delta T_{shear}$ calculated by the Eq. (1).

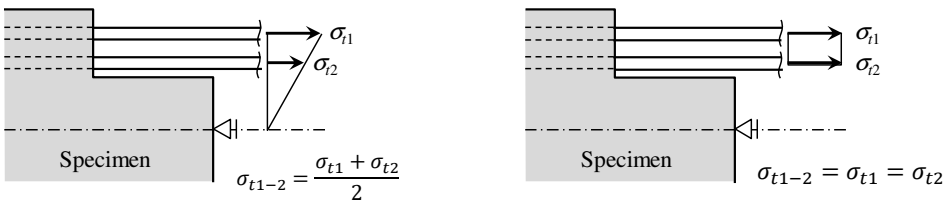


(a) For specimens in Ref.4 and Ref.7 (b) For specimens in Ref.9

Fig. 13 – Assumption of tensile stress in longitudinal bars

When $\Delta T_{local}$ /$\Delta T_{shear}$ is larger than 1.0, a calculated failure mode is the side split mode, and the experimental value should be evaluated by using $\Delta T_{shear}$. As shown in Fig.14, the experimental values of the



 



specimens, $\Delta T_{local}/\Delta T_{shear}$ of which are larger than 1.0, almost agree with $\Delta T_{shear}$. When $\Delta T_{local}/\Delta T_{shear}$ is smaller than 1.0, the calculated failure mode is the local bond failure, and the experimental values should be evaluated by using ${}_{top}\tau_{bu}$ or ${}_{lateral}\tau_{bu}$. Fig.15 shows a comparison between the experimental values and calculated values of bond strengths. The vertical axis is the experimental value ($\tau_{bMAX}$) which is the maximum of bond stress. The horizontal axis is the calculated value ($\tau_{bu\text{-}local}$) which is bond strength (${}_{top}\tau_{bu}$ or ${}_{lateral}\tau_{bu}$) of calculated split mode. The split mode is calculated by comparing bond capacities of $\Delta T_{top}$ and $\Delta T_{lateral}$, and it is the mode corresponded with smaller capacity. Fig.15 shows results of fourteen specimens $\Delta T_{local}/\Delta T_{shear}$ of which are smaller than 1.10. The calculated split mode of one specimen is the lateral split mode, and those of thirteen specimens are the top split mode. As shown in Fig.15, the experimental values of the bond strengths almost agree with the calculated values.

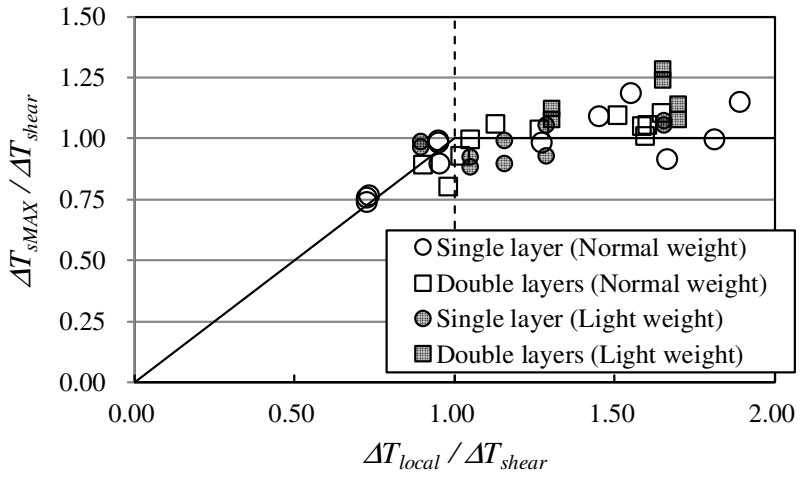


Fig. 14 – Comparison of total bond capacity between test results and calculation

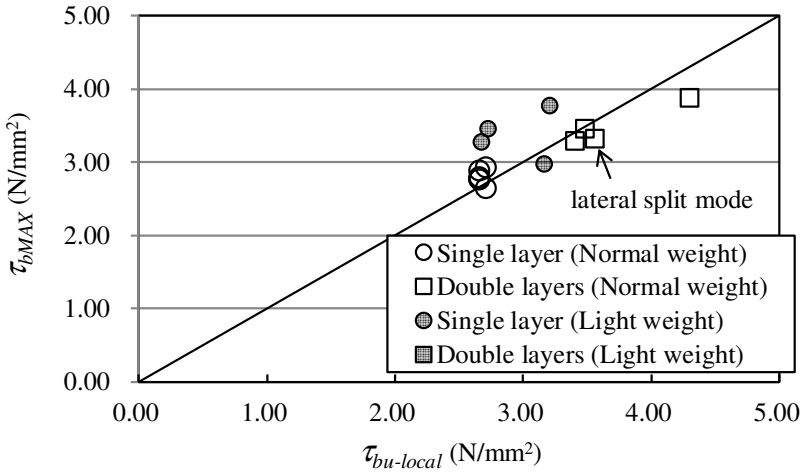


Fig. 15 – Comparison of bond strength between test results and calculation ($\Delta T_{local}/\Delta T_{shear}$ <1.10)

As discussed above, a specimen can have capacity of $\Delta T_{shear}$ if the bond stresses around the any longitudinal bars do not exceed the bond strength. Therefore, it is considered that we can prevent the local



 



bond failure by using the total bond capacity ($\Delta T_{shear}$) and the bond strength such as ${}_{top}\tau_{bu}$ and ${}_{lateral}\tau_{bu}$. For example, in a case of a beam having both the longitudinal bars terminated in the span and the bars passing through the span, we can check the shear capacity by applying $\Delta T_{shear}$ to formulas of shear capacities as is in the Inelastic Concept Guidelines [2] or the previous paper [3]. And we can prevent the local bond failure under shear force which is lower than the shear capacity by checking the bond stress of each bar does not exceed the bond strength.

## 5. Conclusion

When deformed bars embedded in concrete are pulled, an entire bond failure or a local bond failure can occur. The methods for calculating the capacity concerned with the entire bond failure (total bond capacity $\Delta T_{shear}$) and the bond strength of the local bond failure (${}_{top}\tau_{bu}$ and ${}_{lateral}\tau_{bu}$), are proposed in the previous studies [3, 4, 7]. In this paper, the effect of concrete weight was considered in those calculation methods. Calculated values and failure modes according to the proposed method successfully agreed with the results of pull-out tests of deformed bars embedded in concrete. This result implies that the local bond failure can be prevented by using the total bond capacity ($\Delta T_{shear}$) and the bond strength such as ${}_{top}\tau_{bu}$ and ${}_{lateral}\tau_{bu}$.

## 6. References

[1] Architectural Institute of Japan (2018): *AIJ Standard for Structural Calculation of Reinforced Concrete Structure*, Architectural Institute of Japan, (in Japanese).

[2] Architectural Institute of Japan (1999): *Design Guidelines for Earthquake Resistant Reinforced Concrete Buildings Based on Inelastic Displacement Concept,* Architectural Institute of Japan, (in Japanese).

[3] Nishimura K., Ichinose T., and Onishi N. (2016): Consideration on Side-Splitting Bond Strength of R/C Beam with Multi-Layered Reinforcement, *Journal of Structural and Construction Engineering (Transactions of AIJ)*, Vol.81, No.729, pp.1903-1912, (in Japanese).

[4] Nishimura K., and Onishi N. (2018): Experimental Study on Bond Strength of Tension Reinforcing Bars of Different Development Lengths, *Journal of Structural and Construction Engineering (Transactions of AIJ)*, Vol.83, No.743, pp.155-165, (in Japanese).

[5] Ito A., Hasegawa K., Suzuki Y., Takahashi S., and Ichinose T. (2013): Splitting Bond Strength of RC Beam of Which Second Layer Bars are Cut Off, *Journal of Structural and Construction Engineering (Transactions of AIJ)*, Vol.78, No.690, pp.1477-1484, (in Japanese).

[6] Urata K., Murata Y., Iihoshi F., Kono S. Konishi J., Obara T., Nakaune Y., Ohmura T., and Mukai D. (2018): Pull-out Failure of Curtailed Second Layer Longitudinal Reinforcement, Part 2, *Summaries of Technical Papers of Annual Meeting*, Architectural Institute of Japan, Structures IV, pp.97-98, (in Japanese).

[7] Nishimura K., and Kawazu M. (2019): Experimental Study on Local Bond Failure of Tension Reinforcing Bars Embedded in Concrete, *Journal of Structural and Construction Engineering (Transactions of AIJ)*, Vol.84, No.762, pp.1103-1113, (in Japanese).

[8] Masuda, H., Tsuihiji, K., Takagi, H., and Kanoh, Y. (1994): Splitting-Bond Failure at Inner Rebars of Double-Layered Longitudinal Reinforcements, Part 3 Outlines of Test and Test Results, *Summaries of Technical Papers of Annual Meeting*, Architectural Institute of Japan, C, Structures II, pp.645-646, (in Japanese).

[9] Ohyado, M., Iwakura, T., Kanakubo, T., Hirosawa, M., Fujisawa, M., and Sonobe, Y. (1991): Bond Splitting Strength of Concrete Element with Double-Layer Reinforcing, Part 1 Outline of Experiment and Bond Splitting Strength of Light-Weight Concrete, *Summaries of Technical Papers of Annual Meeting*, Architectural Institute of Japan, C, Structures II, pp.349-350, (in Japanese).



 